Solution of three-dimensional fiber orientation in two-dimensional fiber suspension flows

Kun Zhou, Jianzhong Lin, and Tat Leung Chan

Citation: Phys. Fluids **19**, 113309 (2007); doi: 10.1063/1.2815718
View online: http://dx.doi.org/10.1063/1.2815718
View Table of Contents: http://pof.aip.org/resource/1/PHFLE6/v19/i11
Published by the American Institute of Physics.

Solution of three-dimensional fiber orientation in two-dimensional fiber suspension flows

Kun Zhou
State Key Laboratory of Fluid Power Transmission and Control, Zhejiang University, Hangzhou 310027, China

Jianzhong Lin[a)]
State Key Laboratory of Fluid Power Transmission and Control, Zhejiang University, Hangzhou 310027, China and College of Metrology Technology and Engineering, China Jiliang University, Hangzhou 310018, China

Tat Leung Chan
Department of Mechanical Engineering, The Hong Kong Polytechnic University, Kowloon, Hong Kong, China

(Received 15 June 2007; accepted 5 October 2007; published online 29 November 2007)

The orientation of fibers in simple two-dimensional flows is investigated. According to different ranges of the Péclet number, Pe, defined as the ratio of a characteristic rotational speed of fibers and the orientational diffusivity, three methods are developed: characteristic method for $\mathrm{Pe}=\infty$, regular perturbation method for $\mathrm{Pe}\gg 1$, and spectral method for everything else. All the methods subtly utilize the evolving solution of the rotational dynamics of fibers, which is also given in this paper. Especially, the adoption of spherical harmonics in the spectral method eliminates the singularity of the Fokker–Planck equation in spherical coordinates, and provides high precision and efficiency. The evolving solution of orientation distribution with $\mathrm{Pe}=\infty$ is obtained through the solution of rotational dynamics. Using a regular perturbation method, the solution of orientation distribution with $\mathrm{Pe}=\infty$ is extended for the condition of $\mathrm{Pe}\gg 1$. This paper provides systematical and high efficient techniques to deal with the fiber orientation. © *2007 American Institute of Physics*.
[DOI: 10.1063/1.2815718]

I. INTRODUCTION

Fiber suspension flows are significant for both scientific research and industrial application. A fiber is a slender body, and it can be treated as a high aspect ratio cylinder or ellipsoid. The aspect ratio r_c is generally defined as the ratio of the maximum and the minimum characteristic sizes of a body. Because of fiber's high aspect ratio, fiber suspensions show obvious anisotropy. The anisotropy is usually treated by an ensemble average method. In the method, a fiber is endowed with an orientation distribution ψ. Then the anisotropic effect of fiber suspensions on flows is depicted by the orientation distribution.

There are two main aspects in the research of fiber suspensions flows. One aspect is to investigate the movement of fibers in flows. This research field belongs to low Reynolds number hydrodynamics.[1] Because fibers are very small, the flow around a fiber can usually be seen as a creeping flow in moving coordinates aligned with the fiber's mass center. The rotation of fibers has much more important meanings than the translation. A lot of research work has been done on the orientation of fibers in different flows.[2–7] Recently, the orientation of fibers in turbulent flows also involved many investigations.[8–13] The other aspect is to investigate into the new properties of flows caused by the addition of fibers. This research field belongs to rheology. It is basically the additional stress induced by the fiber suspensions, which makes the fiber suspension flows exhibit special rheological properties,[14,15] such as the drag reducing,[16,17] shear thinning,[18] etc. In his serial works,[19–21] Batchelor developed a well-known model about the additional stress $\boldsymbol{\tau}_a$,

$$\tau_a = \mu_f\left(\langle \boldsymbol{pppp}\rangle - \tfrac{1}{3}\boldsymbol{I}\langle \boldsymbol{pp}\rangle\right):\varepsilon,$$

$$\langle \boldsymbol{pppp}\rangle = \oint \boldsymbol{pppp}\,\psi d\boldsymbol{p}, \tag{1}$$

$$\langle \boldsymbol{pp}\rangle = \oint \boldsymbol{pp}\,\psi d\boldsymbol{p}$$

in which $\boldsymbol{p}$ is the fiber orientation vector, ε is the deformation rate tensor, and $\boldsymbol{I}$ is the second order unit tensor. The model contains an apparent viscosity μ_f, which is related to the aspect ratio and the volume fraction of the fibers. Shaqfeh and Fredrickson[22] derived an expression for the apparent viscosity of semidilute suspension using a diagrammatic renormalization technique.

It should be mentioned that there is another popular way to deal with the orientation of fibers. Instead of directly solving the fiber orientation distribution ψ to obtain the second order and the fourth order orientation tensor, $\langle \boldsymbol{pp}\rangle$ and $\langle \boldsymbol{pppp}\rangle$, new evolution equations about $\langle \boldsymbol{pp}\rangle$ and $\langle \boldsymbol{pppp}\rangle$ are developed.[23,24] But an artificial relationship between $\langle \boldsymbol{pp}\rangle$

a)Author to whom correspondence should be addressed. Electronic mail: mecjzlin@public.zju.edu.cn.

and $\langle \boldsymbol{pppp} \rangle$ must be given to close the new evolution equations. The basic idea is the same as that in the famous turbulence model theory. The approximation inevitably encounters the closure problem. Various closure approximations have been developed.[25–27] Under some specific flow conditions, some closure approximations agree with the experiments very well.[28] However, under some other specific flow conditions, the closure approximations give incorrect results.[29–31] Albeit the closure approximations generally have relatively higher computational efficiency than the distribution based method, yet the former has lower precision and narrower field of application compared with the latter.

In this paper, we first review Jeffery's equation[32] about the rotation of fibers in Stokes flow. Then, we discuss the relationship between the rotational dynamics of fibers and the orientation distribution of fibers. It is demonstrated that rotational dynamical equation is not subordinative to the Fokker–Planck equation, which is used to model the orientation distribution. In Sec. III, the rotational equations of fibers in simple 2D flows are solved. Subsequently, using the fiber rotation solution, three methods (spectral method, characteristics method, and regular perturbation method) are developed to solve the Fokker–Planck equation for the three ranges of Péclet number, respectively. The orientation of fibers in simple 2D flows is systematical treated.

II. BASIC EQUATIONS

A. Deterministic rotational dynamics of fibers

For external flow around a particulate, if the Reynolds number defined as the characteristic length of the particulate and the relative velocity between the particulate and the local fluid is near zero, then the flow can be approximated by the steady Stokes equation.

There are only a few flows around the special shaped particulate that can be analytically solved. The ellipsoidal particulate is one of the most important cases, because the harmonic analysis of the Laplacian can be used to deal with the nonslip boundary condition in an ellipsoidal coordinate system.[33] Meanwhile, the ellipsoid is the generalization of various simpler shapes, i.e., sphere, prolate, and oblate spheroid, etc. A high aspect ratio ellipsoid can also be used to approximate a slender fiber in extreme conditions. Jeffery[32] first studied the motion of an ellipsoid in Stokes flow, and he found that the force acting on the ellipsoid reduces to two couples, one tending to make the ellipsoid adapt to the same rotation as the surrounding fluid, and the other tending to set the ellipsoid with its axes parallel to the principle axes of distortion of the surrounding fluid. The discovery was verified by the subsequent experiment of Taylor.[34] Furthermore, Bretherton[35] extended Jeffery's conclusion to a revolution body, and demonstrated that the orientation of the axis of almost any body of revolution is a periodic function of time in any unidirectional flow. For a fiber, Jeffery's result induces the following equation:

$$\dot{\boldsymbol{p}} = \boldsymbol{\omega} \cdot \boldsymbol{p} + \lambda(\boldsymbol{\varepsilon} \cdot \boldsymbol{p} - \boldsymbol{\varepsilon}:\boldsymbol{ppp}),$$

where $\boldsymbol{p}$ is the unit vector aligned with the fiber axis, the dot over the variable denotes the time derivative, $\boldsymbol{\omega}=(\nabla \boldsymbol{u}^{\dagger} - \nabla \boldsymbol{u})/2$ is the vorticity tensor, $\boldsymbol{\varepsilon}=(\nabla \boldsymbol{u}^{\dagger} + \nabla \boldsymbol{u})/2$ is the deformation rate tensor, $\lambda=(r_c^2-1)/(r_c^2+1)$. It is wothwhile to point out that Dinh and Armstrong[36] obtained a similar model for the fiber orientation evolution using the method of averaging Green's function. Their model can be considered as a simplification of the Jeffery's model.

B. Fiber orientation distribution

According to their experimental results, Folgar and Tucker[37] claimed that the ensemble average of fiber orientation could be simulated by a phenomenological model, the Fokker–Planck equation

$$H\psi = 0 \tag{2}$$

where, the Fokker–Planck operator H is defined as

$$H\psi = \frac{\partial \psi}{\partial t} + \nabla_{\boldsymbol{p}} \cdot (\psi \dot{\boldsymbol{p}} - \boldsymbol{D} \cdot \nabla_{\boldsymbol{p}} \psi). \tag{3}$$

Here, the subscript $\boldsymbol{p}$ in the ∇ operator denotes that the operation is on the fiber orientational configuration space, and it is omitted below for brevity; the second order tensor $\boldsymbol{D}$ is an apparent diffusivity.

The Fokker–Planck equation is a popular model to simulate the probability distribution of a stochastic process. Equation (2) in fact corresponds to a stochastic differential equation about the fiber rotational dynamics

$$d\boldsymbol{p}_s = \dot{\boldsymbol{p}} dt + \boldsymbol{B} d\boldsymbol{W}, \tag{4}$$

in which $d\boldsymbol{W}$ is a multivariate Wiener process, and $\boldsymbol{B}$ satisfies the condition $\boldsymbol{B}\boldsymbol{B}^T=\boldsymbol{D}$. The stochastic part introduces diffusion into the determinant dynamical equation. The diffusion may be caused by Brownian movement, or by the hydrodynamical fluctuation induced by the existence of other fibers or even by turbulence. In this paper, we do not deal with the stochastic differential equation. There are many good relevant monographs, such as Refs. 38 and 39. The determinant dynamical equation corresponds to the nondiffusive Fokker–Planck equation, which is called the Liouville equation in classic mechanics.[40] It seems that there is a broad misunderstanding about the relationship between the fiber rotational dynamical equation and the orientation distribution, for many researchers think that the former is just an adjoint equation of the latter. In fact, the fiber rotational dynamical equation includes much more information than the Fokker–Planck equation. The former describes the system in detail, whereas the latter gives only averaged results.

III. DETERMINISTIC FIBER ROTATIONAL DYNAMICS

In this section, the fiber rotational dynamical equation is solved. The solution is the precondition of the "characteristic spectral method" introduced in the next section, and also provides a simple expression for the nondiffusive orientation distribution. Since the fiber is not stretchable, it is natural to

take spherical coordinates to depict the fiber orientation. A sketch is given in Fig. 1. Meanwhile, we denote $\partial u/\partial y=\dot{\gamma}$, $\partial v/\partial x=k\dot{\gamma}$, $\partial u/\partial x=j\dot{\gamma}$, and $\partial v/\partial y=-j\dot{\gamma}$, u and v are velocities in the x and y directions, respectively. In the former substitution, the incompressible condition has been taken into consideration. Then the dynamic equation expands to the following form:

$$\dot{\phi}=\tfrac{1}{2}[\lambda(k+1)\cos(2\phi)+k-1-2\lambda j\sin(2\phi)]\dot{\gamma}, \tag{5}$$

$$\dot{\theta}=\tfrac{1}{4}\lambda\sin(2\theta)[2j\cos(2\phi)+(k+1)\sin(2\phi)]\dot{\gamma}. \tag{6}$$

Integrate Eqs. (5) and (6), then

$$\phi=\arctan\left[\left(-2\lambda j+\tanh\left\{\operatorname{arctanh}\left[\frac{\tan(\phi_0)(\lambda k+\lambda-k+1)+2\lambda j}{\sqrt{\Delta}}\right]+\frac{1}{2}\dot{\gamma}t\sqrt{\Delta}\right\}\sqrt{\Delta}\right)(\lambda k+\lambda-k+1)^{-1}\right], \tag{7}$$

$$\theta=\arctan\left[\frac{\sin(\theta_0)\sqrt{2\lambda j\sin(2\phi_0)-\lambda(k+1)\cos(2\phi_0)-k+1}}{\cos(\theta_0)\sqrt{2\lambda j\sin(2\phi)-\lambda(k+1)\cos(2\phi)-k+1}}\right], \tag{8}$$

where θ_0 and ϕ_0 are the initial values, and

$$\Delta=\lambda^2[(k+1)^2+4j^2]-(k-1)^2. \tag{9}$$

The Δ is discriminant to judge the fiber movement: $\Delta>0$ corresponds to asymptotic movement; $\Delta<0$ corresponds to the periodic movement. As for asymptotic movement, the following formula gives the asymptotic angle:

$$\phi_d=\arctan\frac{-2\lambda j\pm\Delta}{\lambda(k+1)+1-k}. \tag{10}$$

The asymptotic angle has two values, one corresponding to an unstable position and the other corresponding to an asymptotic stable position. As for the periodic movement, the following formula gives the period

$$T=\frac{4\pi}{\dot{\gamma}\sqrt{|\Delta|}}. \tag{11}$$

Both the asymptotic angle and the period can be extended to denote the angle corresponding to an extremum of angle velocity in the periodic case and the relaxation period in the asymptotic case, respectively.

The authors[41] presented a detailed derivation and a thorough discussion of the above results. Here, only a few conclusions are reviewed for better understanding of the fiber orientation distribution. Two groups of general fiber orientation orbits are shown in Fig. 2, one for the periodic case and the other for the asymptotic case. The well-known Jeffery orbit is a special instance there of the extremum [the dotted line in Fig. 2(a)] is in the direction of the x axis. Although the orbits clearly depict the fiber's rotational movement, they do not present some novel properties of the evolution of the orientation distribution. Figure 3 shows the evolution of an approximately evenly distributed initial orientation[42] in a simple shear flow, i.e., $k=0$, $j=0$. First, it should be pointed out that the period of orientation distribution is only half of the fiber rotational movement because the two ends of a fiber are identical. In addition, the distribution is symmetric (only for periodic case), so only $1/4T$ is necessary to depict the orientation evolution. As the orbit implies, the distribution in

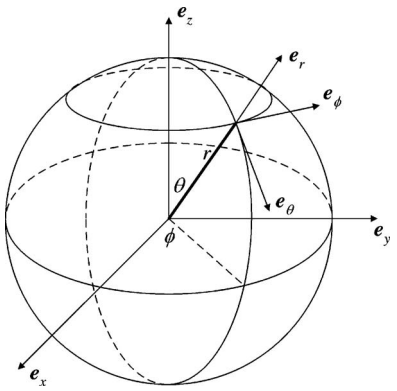

FIG. 1. Schematics of the coordinates. The bold line segment denotes the fiber orientation vector.

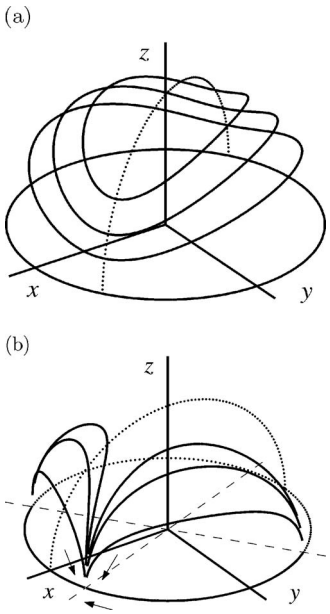

FIG. 2. Typical orientation orbits. (a) Periodic orbits $k=-0.5$, $j=-0.5$; (b) asymptotic orbits $k=0.5$, $j=0.5$.

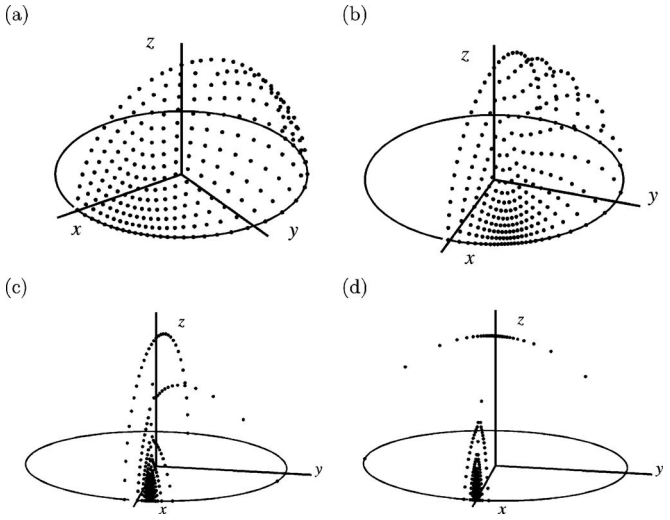

FIG. 3. Orientation evolution of approximately evenly distributed initial orientation in simple shear flow. (a) $1/40T$; (b) $1/20T$; (c) $1/8T$; (d) $1/4T$.

the extremum direction gets the highest value. However, the distribution still gets local extremum other than in the extremum direction during the process of evolution. The conclusion is also true in other flow conditions.

It is a direct thought to evaluate the distribution through a statistic sample of abundant fiber rotational orbits. There are a lot of works on statistical methods.[43,44] But generally speaking, the statistic method has relatively lower computational efficiency and accuracy than a distribution based method. That is because on the one hand the orientation distribution varies severely, which makes the sample difficult; on the other hand, the statistical method takes too many efforts to obtain much unnecessary information, because the distribution based method does not distinguish the movement of different fibers in detail, but the statistic method does. In the next sections, we will show how to subtly utilize the solution of fiber rotation to obtain the distribution solution.

IV. SPECTRAL METHOD

In spherical coordinates, a normal finite difference or finite element method will encounter great numerical difficulties near the two pole points, where the CFL number gets extraordinarily large and the convergence is constrained.[45] In this section, we will present a spectral method that is of high precision and efficiency on the whole sphere. In the spectral method, there are three main steps: First, suppose that the orientation distribution function ψ can be expanded with the base functions of spherical harmonics and undefined coefficients; secondly, use the Galerkin method to obtain a group of equations about the coefficients; finally, solve the equations about the coefficients to obtain the final spectral solution. The detailed derivation is given as below.

Suppose that ψ has an approximation ψ_N in the form of

$$\psi_N = \sum_{n=0}^{N} \sum_{m=-n}^{n} a_{mn}(t) Y_n^m(\phi,\theta), \tag{12}$$

where $Y_n^m(\phi,\theta)$ are the spherical harmonics

$$Y_n^m(\phi,\theta) = \begin{cases} e^{im\phi} P_n^m(\cos\theta), & \text{if } m \geqslant 0 \\ (-1)^m e^{im\phi} P_n^{-m}(\cos\theta), & \text{if } m < 0 \end{cases} \tag{13}$$

and $P_n^m(\cos\theta)$ are the associated Legendre functions. The complex form of $e^{im\phi}$ is just a simple denotation for $\cos(m\phi)$ and $\sin(m\phi)$. Substitute ψ_N into the Fokker–Planck equation, then we have

$$H\psi_N = F_R(\phi,\theta;a_{mn}), \tag{14}$$

where F_R is the residual function.

Define an inner product as

$$(f|g) \equiv \int_0^{\pi} \int_0^{2\pi} fg \sin\theta d\phi d\theta, \tag{15}$$

then the spherical harmonics satisfy the following orthogonal relation:

$$[Y_n^m(\phi,\theta)|Y_k^l(\phi,\theta)] = \begin{cases} 0, & \text{if } n \neq k \text{ or } m \neq l \\ \dfrac{(n+m)!}{(n-m)!} \dfrac{2\delta_m \pi}{(2n+1)}, & \text{if } k = n, l = m \end{cases} \tag{16}$$

where

$$\delta_m = \begin{cases} 2, & \text{if } m = 0 \\ 1, & \text{if } m \neq 0. \end{cases} \tag{17}$$

Take the inner product of both sides of Eq. (2) with Y_k^l and impose an additional condition $(F_R|Y_k^l)=0$ to minimize the residual, then we obtain a series of equations about the undefined coefficients a_{mn},

$$(H\psi_N|Y_k^l) = 0. \tag{18}$$

$H\psi_N$ contains three physically different terms: unsteady term, convective term, and diffusive term. The inner products of the terms with a test function Y_k^l are treated respectively below.

A. Unsteady term

Since the time derivative does not influence the space variables, then according to the orthogonal relation (16) the inner product has the simple expression as

$$(\dot{\psi}_N|Y_k^l) = \frac{(k+l)!}{(k-l)!} \frac{2\delta_l \pi}{(2k+1)} \dot{a}_{lk}. \tag{19}$$

B. Diffusive term

In the Fokker–Planck equation, the diffusivity $\boldsymbol{D}$ is generally a second order tensor. From a mathematical point of view, $\boldsymbol{D}$ is a nonsingular matrix and can always be diagonalized. So it is natural to assume the diffusivity tensor has only nonvanishing diagonal components D_θ and D_ϕ. However, the diffusivities are supposed to be dependent on the fiber orientation distribution.[46,47] Then the Fokker–Planck equation becomes nonlinear and generally needs an iterative solving process. As an approximation, it seems reasonable to assume that the diffusivity is only dependent on the solution of the nondiffusive Fokker–Planck equation. According to this as-

sumption, the diffusivities D_θ and D_ϕ will be functions of $\dot{\theta}$ and $\dot{\phi}$, because the nondiffusive Fokker–Planck equation can be solved in the terms of $\dot{\theta}$ and $\dot{\phi}$ [see Eq. (35)]. Since the solution of $\dot{\theta}$ and $\dot{\theta}$ has been given in the time dependent form, the diffusivities D_θ and D_ϕ can be transformed into the forms that are independent of the coordinates θ and ϕ. Thus the diffusive term in the Fokker–Planck equation has the following form:

$$\nabla \cdot (\boldsymbol{D} \cdot \nabla \psi_N) = \sum_{n=0}^{N} \sum_{m=-n}^{n} \left[-n(n+1)D_\theta + \frac{m^2(D_\theta - D_\phi)}{(\sin\theta)^2} \right] a_{mn}(t) Y_n^m(\cos\theta). \quad (20)$$

It is observed that the above equation is singular at $\theta=0$ and $\theta=\pi$ if D_θ and D_ϕ are not equal. To avoid the singularity, assume D_θ and D_ϕ are equal and can be denoted as D. Therefore, the diffusive term is simplified as follows:

$$\nabla \cdot (\boldsymbol{D} \cdot \nabla \psi_N) = D \sum_{n=0}^{N} \sum_{m=-n}^{n} -n(n+1) a_{mn}(t) Y_n^m(\cos\theta). \quad (21)$$

The above formula is well-known, and it is one of the key features which make the spherical harmonics especially suitable for the Laplacian diffusion problem in spherical coordinates. Then the inner product of the diffusive term with the test function Y_k^l is

$$[\nabla \cdot (\boldsymbol{D} \cdot \nabla \psi_N) | Y_k^l] = -k(k+1) \frac{(k+l)!}{(k-l)!} \frac{2\delta_l \pi}{(2k+1)} a_{lk}(t). \quad (22)$$

C. Convective term

In Eq. (18), the convective term $\nabla \cdot (\dot{\boldsymbol{p}} \psi)$ requires extra treatment. For better understanding, the inner product of the convective term with the test function Y_k^l is expanded below,

$$[\nabla \cdot (\dot{\boldsymbol{p}} \psi_N) | Y_k^l] = \int_0^{\pi} \int_0^{2\pi} \nabla \cdot [(\dot{\theta} \boldsymbol{e}_\theta + \dot{\phi} \boldsymbol{e}_\phi) \times \sum_{n=0}^{N} \sum_{m=-n}^{n} a_{mn}(t) Y_n^m] Y_k^l \sin\theta d\phi d\theta. \quad (23)$$

The double integral does not generally present as a simple form as that in the unsteady term or in the diffusive term, because of the involvement of $\dot{\theta}$ and $\dot{\phi}$. A numerical integration is usually adopted in most spectral methods.

In this paper, we resort to an analytical method to deal with the inner production. The orthogonality of the spherical harmonics is the key point to simplify the inner production. One way to take advantage of the orthogonality is using the theorem of integral by parts, which leads to a group of integral equations involving the unknown inner product term. Another way is to integrate the term directly. Notice that in Eqs. (5) and (6), $\dot{\theta}$ and $\dot{\phi}$ involve only trigonometric functions, and that the spherical harmonics are actually polymers of trigonometric functions; then a direct integration term by term is always feasible. In fact, the direct integration method becomes a typical Fourier analysis process, and the orthogonality of the Fourier series can be used. But the orthogonality of the Fourier series has limited efficiency. There are a great many terms remaining, but the Fourier series are essentially not efficient for the Laplacian problem in spherical coordinates.

Now that we have solved θ and ϕ in the form of time t, the $\dot{\theta}$ and $\dot{\phi}$ are functions of time and independent of θ and ϕ. Then the integral in Eq. (23) can be greatly simplified as the result of the orthogonality of the spherical harmonics. This goal can be achieved after solving the dynamical systems (5) and (6). It seems to be an extra burden to solve the additional dynamical system, but the overwhelming gain is the simplicity of the final results of the double integral. If the initial distribution of the fiber orientation is isotropic, i.e., a fiber has random initial orientation, which is most possible in reality, then the inner product can be simplified further.

Suppose the fiber orientation distribution has an initial value $\psi(0)=1/4\pi$, then

$$\sum_{n=0}^{N} \sum_{m=-n}^{n} a_{mn}(0) Y_n^m(\phi,\theta) = \frac{1}{4\pi}. \quad (24)$$

Take the inner product of both sides of the above equation with Y_k^l and use the orthogonal condition, and it gives

$$a_{mn}(0) = \begin{cases} \dfrac{1}{4\pi}, & \text{if } n=0,\ m=0 \\ 0, & \text{otherwise.} \end{cases} \quad (25)$$

From the above results, it can be deduced that if $a_{nm}(t)$ is not explicitly or implicitly coupled with $a_{00}(t)$, then it will be consistently zero. This conclusion will simplify the analysis greatly.

Suppose $\dot{\theta}$ and $\dot{\phi}$ does not depend on θ and ϕ, then

$$\begin{aligned} &\nabla \cdot [(\dot{\theta} \boldsymbol{e}_\theta + \dot{\phi} \boldsymbol{e}_\phi) \cos(m\phi) P_n^m(\cos\theta)] \\ &\quad = (n-m+1)\dot{\theta} \cos(m\theta) P_{n+1}^m(\cos\theta) \\ &\qquad - [n\dot{\theta} \cos(m\phi) \cos\theta + m\dot{\phi} \sin(m\phi)] P_n^m(\cos\theta) \end{aligned} \quad (26)$$

in which we have chosen $\cos(m\phi)$, the real part of $e^{im\phi}$ in the spherical harmonics. The imaginary part $\sin(m\phi)$ does not exist because of the initial condition (25). Substitute Eq. (26) into Eq. (23), and use the orthogonality between $\cos(m\phi)$ and $\cos(l\phi)$, and it has

$$[\nabla \cdot (\psi_N \dot{\boldsymbol{p}}) | Y_k^l] = \int_0^{\pi} \sum_{n=0}^{N} a_{ln}(t) \{(n-l+1)\dot{\theta}\delta_l P_{n+1}^l(\cos\theta) - [n\dot{\theta}\delta_l \cos\theta] P_n^l(\cos\theta)\} P_k^l(\cos\theta) \sin\theta d\theta. \quad (27)$$

Since the Legendre polymers is in fact the trigonometric series in disguise, then the integral above can be easily evaluated using the trigonometric combination formula and the orthogonal relation of the trigonometric series. It is found

that the integral vanishes if $n+k$ is an even number. The integration can be easily treated by a mathematical software, such as MAPLE. Recall the conclusion that $a_{nm}(t)$ is consistently zero except that it is explicitly or implicitly coupled with $a_{00}(t)$, so only a_{0n} should be taken into consideration. For convenience, we simply denote it as a_n. It is worth stressing that the direct integral method (Fourier series method) mentioned above does not hold the simplicity, within which $a_{mn}(t)$ is coupled with much more nonvanishing terms $a_{kl}(t)$. Generally, the strong coupling slows down the convergence rate of the approximation series and produces stiff equations which is hard to be treated numerically.

D. Dynamical system of coefficients

Substituting the above results of unsteady, diffusive, and convective terms into Eq. (18), produces the dynamical system

$$\begin{bmatrix} \dot{a}_0 \\ \dot{a}_1 \\ \dot{a}_2 \\ \dot{a}_3 \\ \dot{a}_4 \\ \vdots \end{bmatrix} = \begin{bmatrix} 0 & 0 & 0 & 0 & 0 & \cdots \\ -\frac{3}{4}\pi\dot{\theta} & -2D & \frac{3}{32}\pi\dot{\theta} & 0 & \frac{3}{256}\pi\dot{\theta} & \cdots \\ 0 & -\frac{15}{16}\pi\dot{\theta} & -6D & \frac{15}{64}\pi\dot{\theta} & 0 & \cdots \\ -\frac{21}{32}\pi\dot{\theta} & 0 & -\frac{147}{128}\pi\dot{\theta} & -12D & \frac{1617}{4096}\pi\dot{\theta} & \cdots \\ 0 & -\frac{45}{66}\pi\dot{\theta} & 0 & -\frac{1395}{1024}\pi\dot{\theta} & -20D & \cdots \\ \vdots & \vdots & \vdots & \vdots & \vdots & \ddots \end{bmatrix} \begin{bmatrix} a_0 \\ a_1 \\ a_2 \\ a_3 \\ a_4 \\ \vdots \end{bmatrix} \tag{28}$$

subjected to the initial conditions of Eq. (25). It is easy to see that a_0 holds the exact solution $a_0=1/4\pi$, which corresponds to a zero order approximation. In the coefficient matrix on the right-hand side, the elements that are farther and farther away from the diagonal get smaller and smaller. That is because of a weak coupling between faraway orders in the expansion. It is also found that when D is large enough, the matrix is diagonally dominant, which guarantees the numerical stability. We will manifest it in the next section.

E. Numerical solution

1. Error estimation

It is extremely important to estimate different errors in numerical simulations. There are three kinds of errors in a typical spectral method: Truncation error, discretization error, and interpolation error.[45] The interpolation error is the error made by approximating a function by a series of interpolation or collocation points. In this paper, the integral in the inner product is exact, and it is not necessary to approximate the integral by a series of collocation points which is inevitable in the pseudospectral method; so there is no interpolation error in our method at all. As for the present study, the truncation error is the error between the true ψ and the truncated approximation ψ_N, the discretization error is the error between the true a_n and the approximated a_n by neglecting the higher orders in the dynamical system (28).

A small discretization error essentially requires that the dynamical system (28) is stable under small perturbations when truncated at arbitrary order. The dynamical system is linear with the time dependent coefficient matrix. A classic stable analysis is to introduce a new variable to substitute the time and to convert the original system into a one-order higher autonomous dynamical system, and then judge the stability according to the eigenvalues of the new system. The analysis process is too complex for the present study, so we simply evaluate different order truncations to check the stability. Figure 4 gives the two different order approximations of a_1 evolution under the periodic case and asymptotic case,

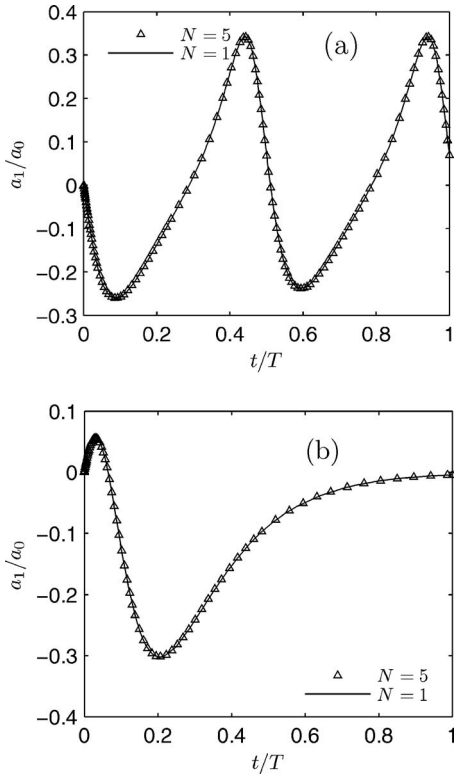

FIG. 4. The a_1 value computed by different truncation orders with Pe=1. (a) Periodic case: $k=-0.5$, $j=-0.5$. (b) Asymptotic case: $k=0.5$, $j=0.5$.

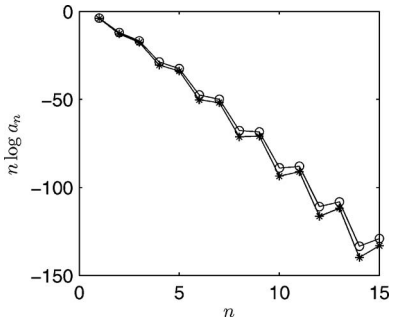

FIG. 5. The magnitude of the coefficients series with Pe=1. The line with circles denotes a periodic case $k=-0.5$, $j=-0.5$; the line with stars denotes an asymptotic case $k=0.5$, $j=0.5$.

respectively. In both cases, there is no observable difference between the low order $N=1$ and high order $N=5$ approximations. This means that the discretization error is very small. To better illustrate the quick convergence of the coefficient series, Fig. 5 gives the relative magnitude of the coefficient series. It is found that the coefficients fluctuate between even and odd orders; they converge at the average order $\mathcal{O}[\exp(-k_a/n)]$, where k_a is an average slope rate of $k_a=n\log a_n+(n+1)\log a_{n+1}/2$. When n is small, the coefficient series converge very fast, when n approaches infinity, and the convergence rate of the series approaches zero. The convergence rate also relies on the Péclet number (defined as $\mathrm{Pe}=|\dot{\gamma}|\sqrt{|\Delta|}/D$ in this paper). The smaller the Péclet number, the faster the series converges (see Fig. 6).

A small truncation error requirement is directly related to the convergence rate of the coefficients series a_n. A higher order of convergence means adopting fewer terms to satisfy the prescribed error demand. The two subfigures of Fig. 7 show the different order approximations of the orientation distribution in a periodic case and an asymptotic case, respectively. In Fig. 7(a) it shows that the first order approximation overestimates the maximum of the distribution by about 20% and overlooks some details, i.e., the small valleys before the peaks which is presented in higher order approximations. Recalling the nondiffusive scattered points picture of the distribution evolution in Fig. 3, it shows that the distribution gets the maximum along $\phi=0$ at time $1/4T$, and it also implies that the distribution is not monotonically increasing or decreasing, which is coincident with the results

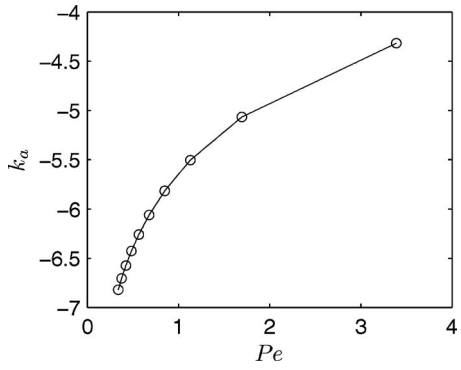

FIG. 6. Average convergence rate under different Péclet numbers.

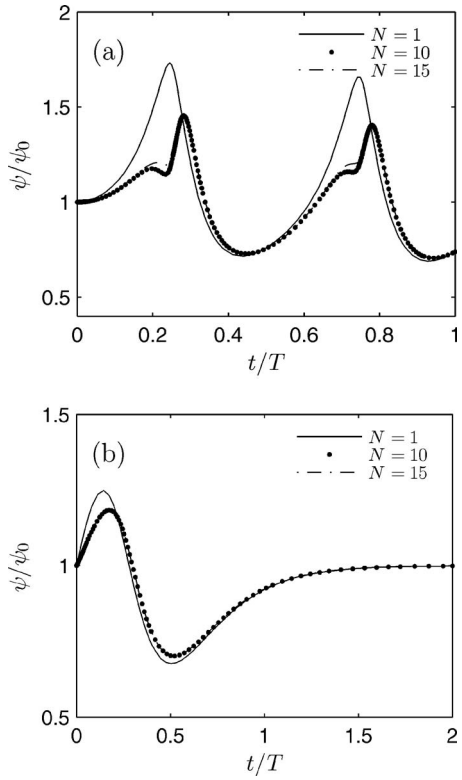

FIG. 7. Different order approximations of the evolution of orientation distribution. (a) Periodic case: $k=0$, $j=0$; $\phi_0=0$, $\theta_0=\pi/3$. $\phi_0=0$ is at the extremum direction. (b) Asymptotic case: $k=0.5$, $j=0.5$; $\phi_0=-0.27\pi$, $\theta_0=\pi/3$. $\phi_0=-0.27\pi$ is very close to the unstable asymptotic direction $\phi_d=-0.30\pi$.

in Fig. 7(a). In Fig. 7(b), the first order approximation only deviates the high order approximations a little bit, while the tenth order and the fifteenth order approximations are almost the same. Although the distribution evolution is investigated only at one space point in both cases, the orientation distribution evolution at the specified point undergoes almost the greatest changes (compared with points of the same ϕ coordinate). It is believed that the tenth order approximation will give very good results over the entire configuration space. When the distribution is smooth enough, the first order approximation is precise enough, which has the analytical form

$$a_1=-\frac{3}{16}\exp(-2Dt)\int_0^t \dot{\theta}\exp(2Ds)ds. \tag{29}$$

It can be easily evaluated using a numerical integration method.

2. Orientation distribution

We have shown some properties of the orientation distribution when discussing the approximation error in the last subsection. Here we will have more detailed discussions. All the solutions are given by the tenth order approximation and are considered to be accurate. Figure 8 shows the orientation distribution under different Péclet numbers for periodic and asymptotic cases. In the two cases, the distributions become

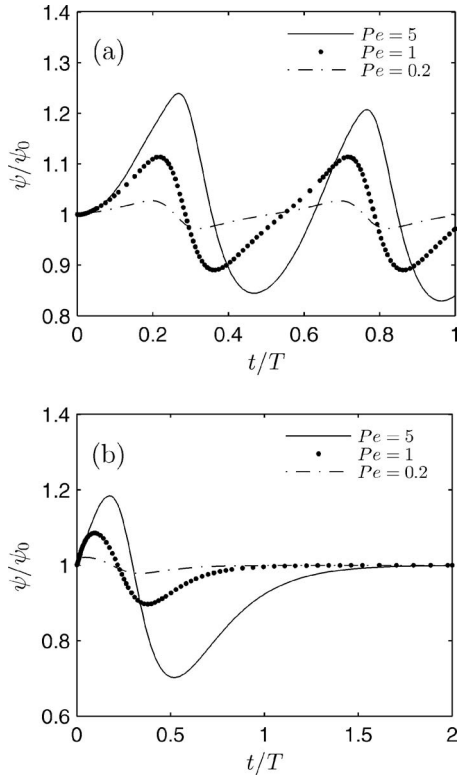

FIG. 8. The evolution of orientation distribution with different Péclet numbers. (a) Periodic case: $k=-0.5$, $j=-0.5$; $\phi_0=0.18\pi$, $\theta_0=\pi/3$. $\phi_0=0.18\pi$ is at the extremum direction. (b) Asymptotic case: $k=0.5$, $j=0.5$; $\phi_0=-0.27\pi$, $\theta_0=\pi/3$. $\phi_0=-0.27\pi$ is very close to the unstable asymptotic direction $\phi_d=-0.30\pi$.

flatter when decreasing the Péclet number, which coincides with the physical intuition, i.e., higher diffusion leading to more homogeneous distribution.

The distribution in Fig. 8(a) corresponds to deterministic periodic rotation of fibers. It is obvious that the distribution is not precisely periodic any more. In fact, the distribution relaxes to a quasiperiodic "constant state" after a relaxation time T_r. The relaxation time is determined by the Péclet number. The higher the Péclet number, the longer the relaxation time. It seems to be a proper way to define the relaxation time as $T_r=\mathrm{Pe}\times T$. It is also found that the peak of the distribution shifts to the left when decreasing the Péclet number. This lag effect may also be seen as the result of the relaxation time difference. Figure 8(a) only gives the distribution evolution at the point $\phi_0=0.18\pi$, $\theta_0=\pi/3$. Numerical solution at other points (not shown in the paper) manifests that the orientation is almost homogeneously distributed along the ϕ direction, while it is single-peak distributed along the θ direction, and especially, the distribution at $\theta_0=0$ and $\theta_0=\pi/2$ has a constant value $1/4\pi$ all the time. The results seem a little peculiar, because the diffusion should not suppress the distribution fluctuation completely. It is found that the peculiarity originates from the homogeneous initial distribution $1/4\pi$ that we have taken. Because of that, the variable ϕ has been canceled in the spherical harmonics, and only θ is left in the dynamical system (28). However, $\dot{\theta}$ is zero at $\theta_0=0$ and $\theta_0=\pi/2$, so the distribution is constant there.

The distribution in Fig. 8(b) corresponds to the deterministic asymptotic rotation of fibers. It is found that the distribution approaches the homogeneous initial value after the relaxation time. This is very different from the nondiffusive distribution, which is expected to decrease to zero except at the stable asymptotic point where it will blow up. First increasing and then decreasing the behavior of the distribution at the transitional interval is the competitive result of the convective and the diffusive effects. Near the unstable asymptotic direction, the distribution tends to increase with time. However, the distribution tends to decrease with time next to the stable asymptotic direction. Since the point $\phi_0=-0.27\pi$ is very close to the unstable asymptotic direction $\phi_d=-0.30\pi$, the distribution presents the behavior of first increasing and then decreasing in the transitional interval. Because of the same reason as for the periodic case, the distribution is constant all the time at $\theta_0=0$ and $\theta_0=\pi/2$.

V. CHARACTERISTIC METHOD

A. Nondiffusive solution of the orientation distribution

The spectral method we have presented has the merits of good precision and high computational efficiency.[48] But as we have pointed out in Sec. IV E 1, the spectral method cannot deal with the problems under very high Péclet number, especially, the Péclet number being infinite, i.e., nondiffusion condition, which is also very important in theoretical research and application. However, we have demonstrated that the fibers' rotational dynamics is equivalent to the orientation distribution in the sense of the weak solution of the distribution. Since the deterministic rotational equations of fibers have been solved in Sec. III, there should be some simple way to obtain the distribution solution. Notice that the nondiffusive Fokker–Planck equation in spherical coordinates has the form

$$\frac{\partial\psi}{\partial t}+\frac{\cos\theta}{\sin\theta}\dot{\theta}\psi+\dot{\theta}\frac{\partial\psi}{\partial\theta}+\frac{\dot{\phi}}{\sin\theta}\frac{\partial\psi}{\partial\phi}=0. \tag{30}$$

It is a first order partial differential equation (PDE), which is always solved by the characteristic method.[49] Using the characteristic method, the corresponding characteristic equations are

$$\frac{d}{ds}t(s)=1, \tag{31}$$

$$\frac{d}{ds}\theta(s)=\dot{\theta}, \tag{32}$$

$$\frac{d}{ds}\phi(s)=\frac{\dot{\phi}}{\sin\theta}, \tag{33}$$

$$\frac{d}{ds}\psi_0(s)=-\frac{\cos\theta}{\sin\theta}\dot{\theta}\psi_0. \tag{34}$$

Substitute Eqs. (31) and (32) into Eq. (34), and then integrate the latter, the result is

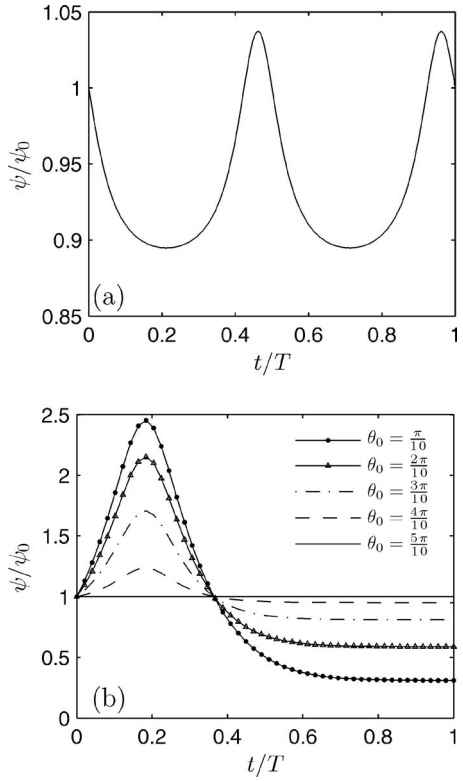

FIG. 9. Nondiffusive orientation distribution evolution along the characteristics. (a) Periodic case: $k=-0.5$, $j=-0.5$; $\phi_0=\pi/2$, $\theta_0=\pi/3$. (b) Asymptotic case: $k=0.5$, $j=0.5$; $\phi_0=0.67\pi$.

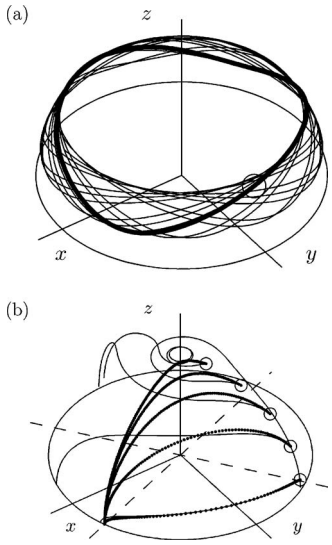

FIG. 10. The characteristics and orbits (corresponding to Fig. 9). (a) $k=-0.5$, $j=-0.5$; $\phi_0=\pi/2$, $\theta_0=\pi/3$. The closed bold line denotes a periodic orbit. The circles indicate the initial position of the characteristic. The slim line denotes the characteristic after the time of $10T$. It exhibits chaotic behavior in the same θ bandwidth with the orbit. (b) $k=0.5$, $j=0.5$; $\phi_0=0.67\pi$. The dotted lines denote the asymptotic orbits, the solid lines denote the characteristics. The little circles denote the starting points of orbits and characteristics.

$$\psi_0(t) = C\exp\left(\int_0^t -\frac{\cos\theta}{\sin\theta}\dot{\theta}ds\right) = C\exp\left(\int_{\theta_0}^{\theta} -\frac{\cos\theta}{\sin\theta}d\theta\right) = C\frac{\sin\theta_0}{\sin\theta}, \tag{35}$$

where the integral constant $C=\psi(\theta_0,\phi_0,0)$ is decided by the initial condition.

During the derivation of the characteristic solution, Eq. (33) has not been used. However, the characteristic method gives the solution along the characteristics, and the characteristics are *not* the rotational orbits of fibers. It is Eq. (33) that makes the characteristics and the orbits different. Equation (33) has the formal solution

$$\phi_c = \phi_0 + \int_0^t \frac{1}{\sin\theta(s)}ds. \tag{36}$$

Here, θ is given by Eqs. (7) and (8).

Figure 9 shows examples of orientation distribution evolution along the characteristics in both periodic and asymptotic cases, and Fig. 10 shows the corresponding characteristics. Figure 9(a) shows the distribution is precisely periodic as the fiber's rotation. The distribution gets maximum at the extremum position. However, the corresponding characteristics [Fig. 9(b)] exhibit chaotic behavior. This is because the ϕ coordinate of the characteristic (denoted as ϕ_c below) has changed from the ϕ coordinate of the orientation orbit by a factor $1/\sin\theta$, which leads to the period of ϕ_c does not have a common multiple with 2π any longer. This is a very interesting result and has not been found before, as far as the authors' knowledge. As for an asymptotic case, all characteristics approach the equator, where the distribution approaches constant value. When the characteristics first cross the asymptotic direction ϕ_d, the distribution obtains its maximum. It is worth pointing out that in a statistical method, this kind of distribution can be hardly observed. Since almost all points are attracted to one point in the asymptotic direction, except those initially lying in the asymptotic direction. This can be verified clearly by the picture of the scattered points that we have presented in Sec. III. The asymptotic case is singular, so a statistical method cannot give an accurate solution.

Szeri and Leal[50] have used a so-called double Lagrangian method to obtain the orientation distribution [Eq. (2.10) in their paper]

$$\psi(\theta_0,\phi_0,t) = \psi(\theta_0,\phi_0,0)\frac{\sin\theta_0}{\sin\theta}\left|\frac{\partial(\theta,\phi)}{\partial(\theta_0,\phi_0)}\right|^{-1} \tag{37}$$

where $|\cdot|$ denotes the Jacobian determinant, θ and ϕ are solutions of the rotational orbits of fibers. But the result conflicts with our derivation. We will discuss it in detail below.

According to the theorem of changing variables, it has

$$\int_S \psi(\theta,\phi,t)d\theta d\phi = \int_{S^\star} \psi(\theta_0,\phi_0,t)\left|\frac{\partial(\theta,\phi)}{\partial(\theta_0,\phi_0)}\right| d\theta_0 d\phi_0. \tag{38}$$

Here S and $S^{\star}$ are the initial integral domain and the corresponding transformed integral domain, respectively. The equivalence above exists universally if only the Jacobian determinant is nonzero. Additionally, if θ and ϕ are the solution of rotational orbits, then it has

$$\psi(\theta_0,\phi_0,t)=\psi(\theta,\phi)\left|\frac{\partial(\theta,\phi)}{\partial(\theta_0,\phi_0)}\right|^{-1}. \tag{39}$$

This is the result of the Liouville theorem (p. 366 in Ref. 51): *The volume of an arbitrary region of phase space is conserved if the points of its boundary move according to the canonical equations.* Suppose that the distribution $\psi(\theta,\phi)$ satisfies Eq. (35), then Eq. (39) gives the same result as Eq. (37). Then the conflict arises. Since the characteristics and the orbits of the fibers do not coincide with each other, it is not possible that both Eqs. (35) and (37) are correct. We have used a classic method and only several lines' deduction to obtain the characteristic solution (35), while Szeri and Leal had developed a novel explanation (double Lagrangian method) and used several pages' deduction to obtain the result (37). So we doubt that Szeri and Leal have confounded the orbits and the characteristics somewhere during their calculation. In case we are wrong in explaining the solution (35), the former discussion can be seen as an alternative and simple way to deduce Szeri and Leal's result.

B. Weak diffusive solution of the orientation distribution

It is a natural expectation that the orientation distribution with weak diffusion will only deviate slightly from the orientation distribution without diffusion. Leal and Hinch[52] had taken a regular perturbation method to solve the orientation distribution of fibers in simple shear flow. In this section, we take a similar method to obtain the weak diffusive solution of the orientation distribution in any simple planar flows. According to the weak diffusion assumption, the diffusivity D can be rewritten as ϵD_{ϵ}, where $D_{\epsilon}=D/\epsilon$ has the same order as $\dot{\boldsymbol{p}}$, and $\epsilon \ll 1$ is a small parameter. Suppose that the orientation distribution ψ has the following asymptotic expansion:

$$\psi=\psi_0+\epsilon\psi_1+\epsilon^2\psi_2+\cdots. \tag{40}$$

Here, ψ_0 is the solution of the nondiffusive Fokker–Planck equation (30), ψ_1 and ψ_2, etc. are unknown high order approximations. Inserting the expansion (40) into the Fokker–Planck equation (2) and balancing the same order term of ϵ, we obtain an equation about the first order approximation ψ_1,

$$\frac{\partial\psi_1}{\partial t}=-\nabla\cdot(\dot{\boldsymbol{p}}\psi_1)+D_{\epsilon}\nabla\cdot\nabla\psi_0 \tag{41}$$

in which we have used the condition that ψ_0 satisfies Eq. (30). Recursively, a series of high order approximations can be obtained. All the equations obtained in the recursive approximation process are first order PDEs, and they can be solved by the characteristic method. Besides, the equations have a very useful common property that they all have the same characteristics. It can be easily seen from Eq. (41), which has the same form as that satisfied by ψ_0 except for an additional known term. The additional term does not influence the characteristics at all. This can be proved correct recursively for higher orders.

Since we have obtained the characteristic solution of ψ_0 in the subsection above, inserting it into the characteristic equation of ψ_1, we have

$$\dot{\psi}_1=\frac{\dot{\theta}\cos\theta}{\sin\theta}\psi_1+CD_{\epsilon}\frac{\sin\theta_0}{(\sin\theta)^3}. \tag{42}$$

Subjected to the initial condition $\psi_1(0)=0$, the equation above has the following solution:

$$\begin{aligned}\psi_1(t)&=[\sin\theta(t)-\sin\theta_0]\int_0^t\frac{4CD_{\epsilon}\sin\theta_0}{[\sin\theta(s)-\sin\theta_0]\{3\sin\theta(s)-\sin[3\theta(s)]\}}ds\\&=[\sin\theta(t)-\sin\theta_0]\int_{\theta_0}^{\theta(t)}\frac{4CD_{\epsilon}\sin\theta_0}{(\sin\theta-\sin\theta_0)[3\sin\theta-\sin(3\theta)]\dot{\theta}}d\theta.\end{aligned} \tag{43}$$

According to the assumption above, $D_{\epsilon}/\dot{\theta}$ is $\mathcal{O}(1)$. Under this condition, $\psi_1(t)$ is well-behaved in spite of the singularity of the integral in the equation. Because when $\theta\neq 0$ or $\theta\neq\pi$, it has $3\sin\theta-\sin(3\theta)\neq 0$, then the expression above can be simplified to a model $t\int_0^t s^{-1}ds$. The model converges to zero as t approaching to zero, which can be proved by evaluating the limit, $\lim_{t\to 0}t\int_0^t s^{-1}ds$. In a numerical treatment of $\psi_1(t)$, it is convenient to separate $\psi_1(t)$ into a piecewise function. When $t<\epsilon_0$, let $\psi_1(t)=0$; when $t\leqslant\epsilon_0$, let $\psi_1(t)$ be the form of Eq. (43) except changing the lower integral bound from 0 to ϵ_0, where ϵ_0 is a small threshold value to control the precision of the integral.

It should be pointed out that the regular perturbation solution has some limitations. During the derivation, it is required that D_{ϵ} and $\dot{\theta}$ are the same order of magnitude. But this seems seldom satisfied in practice. When $\dot{\theta}$ is small, the orientation distribution should be large. In the region having a relatively large orientation distribution, the diffusivity may be also large. The limitation of the regular perturbation method originates from the problem itself, which in fact

needs a singular perturbation method to deal with. Using a first order PDE (nondiffusive distribution) to model a second order PDE (weak diffusive distribution) is generally not feasible. Gardiner in his book[38] presented a typical singular perturbation process to solve the Fokker–Planck equation with weak diffusion. We have not applied it to the present problem, however, we suspect that it is feasible to the problem.

VI. CONCLUSION

The orientation distribution of fibers in simple 2D flows is solved by three methods: Characteristic method for $\mathrm{Pe}=\infty$, regular perturbation method for $\mathrm{Pe}\gg 1$, and spectral method for everything else. They can be used to evaluate the orientation of fibers in various 2D flows. As the high precision of these methods, they can also be used to verify various closure approximations of the second and the fourth order tensors, $\langle \boldsymbol{pp} \rangle$ and $\langle \boldsymbol{pppp} \rangle$.

In this paper, a fiber's rotation in simple 2D flows is analytically solved. It is found that the fiber will rotate periodically or turn to an asymptotic direction according to different flow conditions. Since the rotational dynamics of fibers is equivalent to the evolution of orientation distribution with $\mathrm{Pe}=\infty$ in the sense of the weak solution of the distribution, which is shortly demonstrated in this paper, then the orientation distribution is obtained from the solution of the rotational dynamics by the characteristic method.

A highly precise and efficient spectral method is developed for $\mathrm{Pe}\leqslant \mathcal{O}(1)$. The application of spherical harmonics as the base functions of the spectral method eliminates the singularity of the Fokker–Planck equation in spherical coordinates, which is unavoidable in other numerical methods, such as finite difference method and finite element method. Meanwhile, the creative application of the evolution solution of fiber's rotational dynamics in the spectral method has greatly simplified the computation. Even an analytical first order spectral approximation is obtained. High order approximations are given by a well-behaved dynamical system, which can be easily computed to give precise results for various specific planar suspension flows.

A regular perturbation solution is given for $\mathrm{Pe}\gg 1$, which covers the gap of the Péclet number between $\mathrm{Pe}\leqslant \mathcal{O}(1)$ and $\mathrm{Pe}=\infty$. The applicable conditions of the regular perturbation solution are also discussed.

ACKNOWLEDGMENTS

The research is supported by the National Natural Science Foundation of China Grant No. 10632070.

[1] J. Happel and H. Brenner, *Low Reynolds Number Hydrodynamics* (Prentice-Hall, Englewood Cliffs, NJ, 1965).
[2] S. B. Chen and L. Jiang, "Orientation distribution in a dilute suspension of fibers subject to simple shear flow," Phys. Fluids **11**, 2878 (1999).
[3] Z. H. Wan and J. Z. Lin, "Hydrodynamic instability of semi-concentration fiber suspensions between two rotating coaxial cylinders," Int. J. Nonlinear Sci. Numer. Simul. **5**, 211 (2004).
[4] J. Z. Lin, X. Shi, and Z. S. Yu, "The motion of fibers in an evolving mixing layer," Int. J. Multiphase Flow **29**, 1355 (2003).
[5] J. Z. Lin, W. F. Zhang, and Z. S. Yu, "Numerical research on the orientation distribution of fibers immersed in laminar and turbulent pipe flows," J. Aerosol Sci. **35**, 63 (2004).
[6] T. Nishinura, K. Yasuda, and K. Nakamura, "Orientation behaviour of fibers in suspension flow through a branching channel," J. Non-Newtonian Fluid Mech. **73**, 279 (1997).
[7] J. Z. Lin, X. Shi, and Z. J. You, "Effects of the aspect ratio on the sedimentation of a fiber in newtonian fluids," J. Aerosol Sci. **34**, 909 (2003).
[8] J. Z. Lin, K. Sun, and J. Lin, "Distribution of orientations in fiber suspension flowing in a turbulent boundary layer," Chin. Phys. Lett. **22**, 3111 (2005).
[9] J. Z. Lin, S. L. Zhang, and J. A. Olson, "Effect of fibers on the flow property of turbulent fiber suspensions in a contraction," Fibers Polym. **18**, 60 (2007).
[10] J. A. Olson, I. Frigaard, C. Chan, and J. P. Hamalainen, "Modeling a turbulent fibre suspension flowing in a planar contraction: The one-dimensional headbox," Int. J. Multiphase Flow **30**, 51 (2004).
[11] M. Parsheh, M. L. Brown, and C. K. Aidun, "On the orientation of stiff fibres suspended in turbulent flow in a planar contraction," J. Fluid Mech. **545**, 245 (2005).
[12] L. X. Zhang, J. Z. Lin, and T. L. Chan, "Orientation distribution of cylindrical particles suspended in a turbulent pipe flow," Phys. Fluids **17**, 093105 (2005).
[13] S. L. Zhang, J. Z. Lin, and W. F. Zhang, "Numerical research on the fiber suspensions in a turbulent T-shaped branching channel flow," Chin. J. Chem. Eng. **15**, 30 (2007).
[14] R. B. Bird, R. C. Armstrong, and O. Hassager, *Dynamics of Polymeric Liquids*, 2nd ed. (Wiley, New York, 1987), Vol. 1.
[15] R. B. Bird, O. Hassager, R. C. Armstrong, and C. F. Curtiss, *Dynamics of Polymeric Liquids*, 2nd ed. (Wiley, New York, 1987), Vol. 2.
[16] J. M. J. Dentoonder, M. A. Hulsen, G. D. C. Kuiken, and F. T. M. Nieuwstadt, "Drag reduction by polymer additives in a turbulent pipe flow: Numerical and laboratory experiments," J. Fluid Mech. **337**, 193 (1997).
[17] J. S. Paschkewitz, Y. Dubief, C. D. Dimitropoulos, E. S. G. Shaqfeh, and P. Moin, "Numerical simulation of turbulent drag reduction using rigid fibres," J. Fluid Mech. **518**, 281 (2004).
[18] M. Manhart, "Rheology of suspensions of rigid-rod like particles in turbulent channel flow," J. Non-Newtonian Fluid Mech. **112**, 269 (2003).
[19] G. K. Batchelor, "The stress system in a suspension of force-free particles," J. Fluid Mech. **41**, 545 (1970).
[20] G. K. Batchelor, "Slender-body theory for particles of arbitrary cross-section in Stokes flow," J. Fluid Mech. **44**, 419 (1970).
[21] G. K. Batchelor, "The stress generated in a non-dilute suspension of elongated particles by pure straining motion," J. Fluid Mech. **46**, 813 (1971).
[22] E. S. G. Shaqfeh and G. H. Fredrickson, "The hydrodynamic stress in a suspension of rods," Phys. Fluids A **2**, 7 (1990).
[23] E. J. Hinch and L. G. Leal, "Constitutive equations in suspension mechanics. Part 1. General formulation," J. Fluid Mech. **71**, 481 (1975).
[24] E. J. Hinch and L. G. Leal, "Constitutive equations in suspension mechanics. Part 2. Approximate forms for a suspension of rigid particles affected by Brownian rotations," J. Fluid Mech. **76**, 187 (1975).
[25] S. G. Advani and C. L. Tucker III, "Closure approximations for three-dimensional structure tensors," J. Rheol. **34**, 367 (1990).
[26] J. S. Cintra and C. L. Tucker III, "Orthotropic closure approximations for flow-induced fiber orientation," J. Rheol. **39**, 1095 (1995).
[27] K. H. Han and Y. T. Im, "Modified hybrid closure approximation for prediction of flow-induced fiber orientation," J. Rheol. **43**, 569 (1999).
[28] M. Parsheh, M. L. Brown, and C. K. Aidun, "Investigation of closure approximations for fiber orientation distribution in contracting turbulent flow," J. Non-Newtonian Fluid Mech. **136**, 38 (2006).
[29] M. C. Altan and B. N. Rao, "Closed-form solution for the orientation field in a center-gated disk," J. Rheol. **39**, 581 (1995).
[30] L. Tang and M. C. Altan, "Entry flow of fiber suspension in a straight channel," J. Non-Newtonian Fluid Mech. **56**, 183 (1995).
[31] K. A. Ericsson, S. Toll, and J. A. E. Manson, "The two-way interaction between anisotropic flow and fiber orientation in squeeze flow," J. Rheol. **41**, 491 (1997).
[32] G. B. Jeffery, "The motion of ellipsoidal particles immersed in a viscous fluid," Proc. R. Soc. London, Ser. A **102**, 161 (1922).
[33] D. Jackson, "The harmonic boundary value problem for an ellipse or an ellipsoid," Am. Math. Monthly **51**, 555 (1944).
[34] G. I. Taylor, "The motion of ellipsoidal particles in a viscous fluid," Proc. R. Soc. London, Ser. A **103**, 58 (1923).
[35] F. P. Bretherton, "The motion of rigid particles in a shear flow at low Reynolds number," J. Fluid Mech. **14**, 284 (1962).

[36]S. M. Dinh and R. C. Armstrong, "A rheological equation of state for semiconcentrated fiber suspensions," J. Rheol. **28**, 207 (1984).
[37]F. Folgar and C. L. Tucker III, "Orientation behavior of fibers in concentrated suspensions," J. Reinf. Plast. Compos. **3**, 98 (1984).
[38]C. W. Gardiner, *Handbook of Stochastic Methods*, 2nd ed. (Springer-Verlag, New York, 1997).
[39]H. Risken, *The Fokker–Planck Equation: Methods of Solution and Applications*, 2nd ed. (Springer-Verlag, Berlin, 1989).
[40]V. I. Arnold, *Mathematical Methods of Classical Mechanics*, 2nd ed. (Springer-Verlag, New York, 1989).
[41]K. Zhou and J. Z. Lin, "Analytical research on 3D fiber orientation distribution in arbitrary planar flows," J. Zhejiang Univ., Sci. A **8**, 1021 (2007).
[42]It is mathematically impossible to evenly distribute arbitrary points on a sphere, because there are only five regular polyhedra.
[43]K. Chiba, K. Yasuda, and K. Nakamura, "Numerical solution of fiber suspension flow through a parallel plate channel by coupling flow field with fiber orientation distribution," J. Non-Newtonian Fluid Mech. **99**, 145 (2001).
[44]A. J. Szeri and L. G. Leal, "A new computational method for the solution of flow problems of microstructured fluids. Part 2. Inhomogeneous shear flow of a suspension," J. Fluid Mech. **262**, 171 (1994).
[45]J. P. Boyd, *Chebyshev and Fourier Spectral Methods*, 2nd ed. (Dover, New York, 2000).
[46]D. L. Koch, "A model for orientational diffusion in fiber suspensions," Phys. Fluids **7**, 2086 (1995).
[47]E. S. G. Shaqfeh and D. L. Koch, "Orientational dispersion of fibers in extensional flows," Phys. Fluids A **2**, 1077 (1990).
[48]All the computations in this paper cost no more than 10 s of CPU time in a normal PC.
[49]R. Courant, *Methods of Mathematical Physics* (Interscience, New York, 1962), Vol. II.
[50]A. J. Szeri and L. G. Leal, "A new computational method for the solution of flow problems of microstructured fluids. Part 1. Theory," J. Fluid Mech. **242**, 549 (1992).
[51]W. Greiner, *Classical Mechanics: System of Particles and Hamiltonian Dynamics* (Springer-Verlag, New York, 2003).
[52]L. G. Leal and E. J. Hinch, "The effect of weak Brownian rotation on particles in shear flow," J. Fluid Mech. **46**, 685 (1971).